

Supporting Information

A bio-inspired, hierarchically porous structure with decoupled fluidic transportation and evaporative pathway toward high-performance evaporation

Jianguo Li,^{1a} Chaoji Chen,^{1a} Wentao Gan,^{1a} Zhihan Li,¹ Hua Xie,¹ Miaolun Jiao,¹ Shaliang Xiao,¹ Hu Tang,¹ Liangbing Hu^{1*}

1. Department of Materials Science and Engineering, University of Maryland, College Park, Maryland, 20742

Corresponding author: binghu@umd.edu

^aThese authors contributed equally to this work.

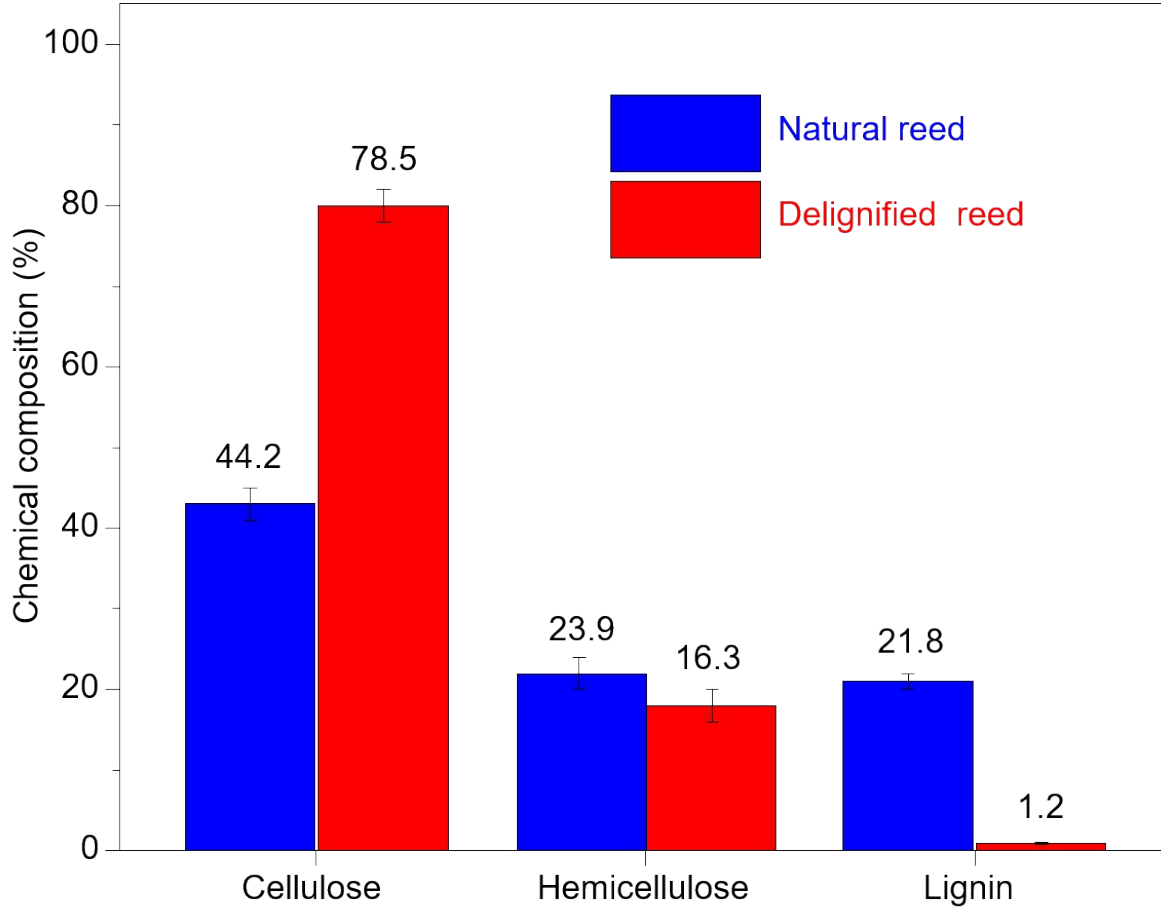


Figure S1. The chemical compositions of the natural and delignified reeds. The delignification treatment completely removes lignin and increases the relative cellulose content. The chemical composition change can promote the hydrophilicity of the reed due to the removal of hydrophobic lignin and the retention of hydrophilic cellulose.

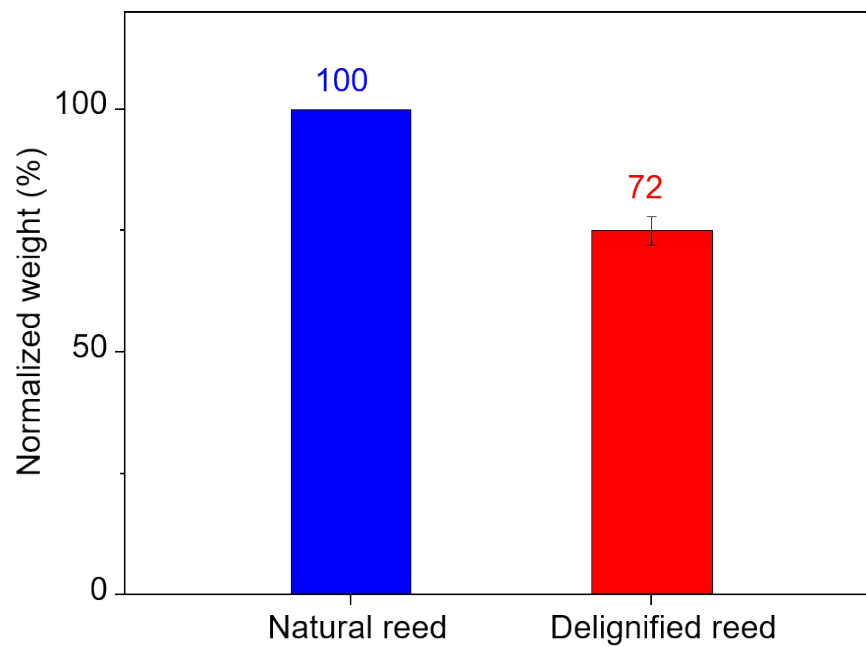


Figure S2. Delignification leads to a decrease of weight from the natural reed to delignified reed, which is an indicator that a large amount of lignin has been removed.

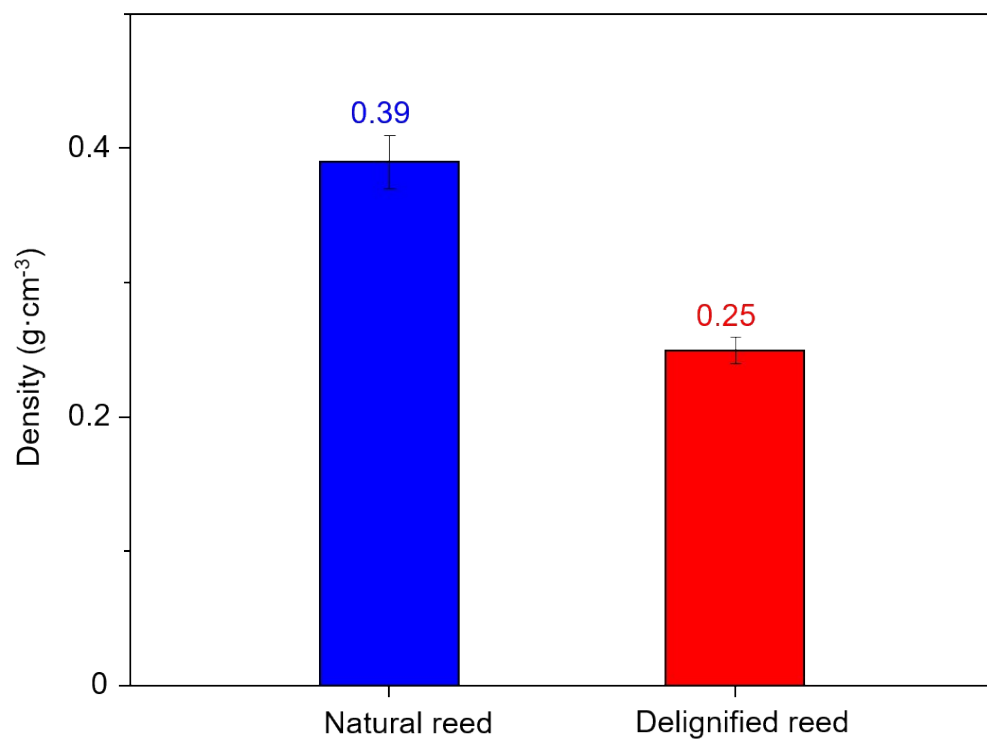


Figure S3. Density of the natural and delignified reeds. The delignified reed shows a lower density, which is evidence of the more porous structure.

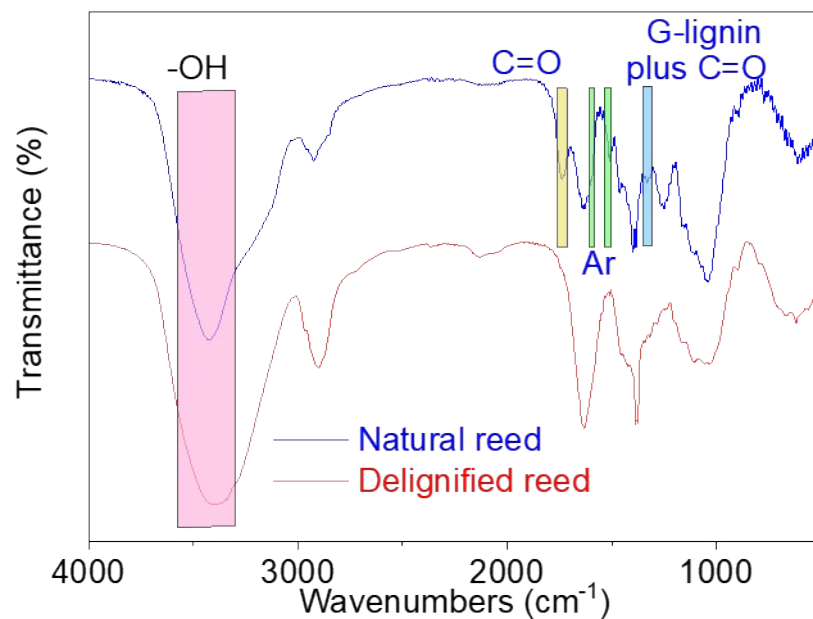


Figure S4. FT-IR results of the natural and delignified reeds. After delignification, most of the functional groups associated with lignin are eliminated.

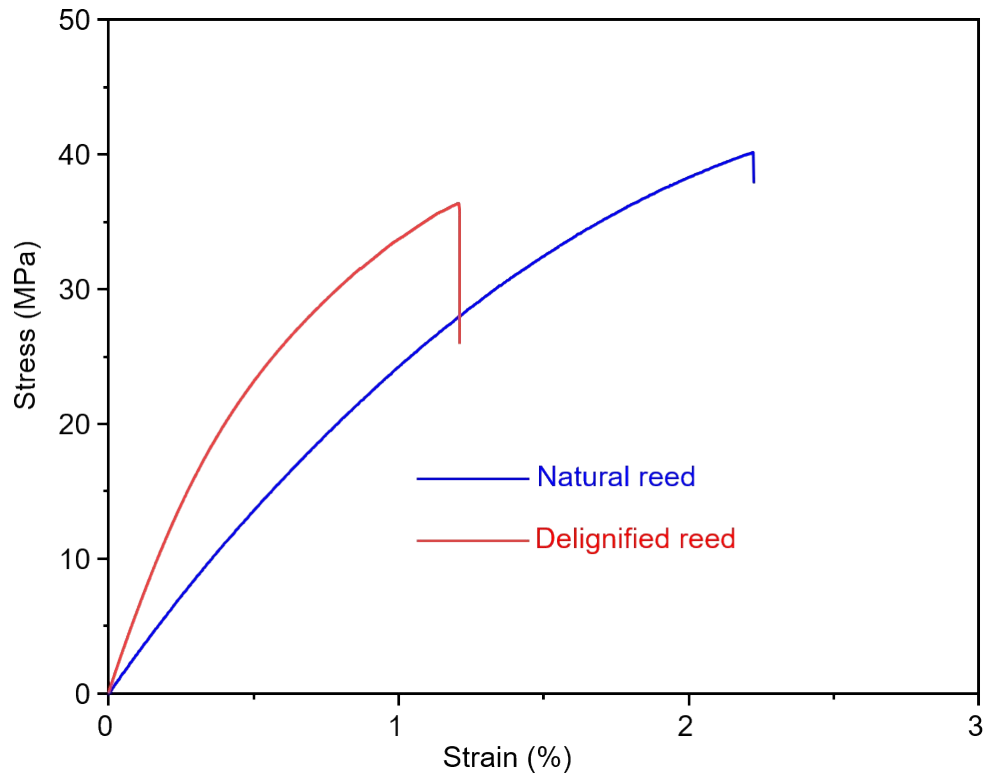


Figure S5. Tensile stress-strain curves. The delignified reed features slightly lower stress, which may be due to its lower density than natural reed.

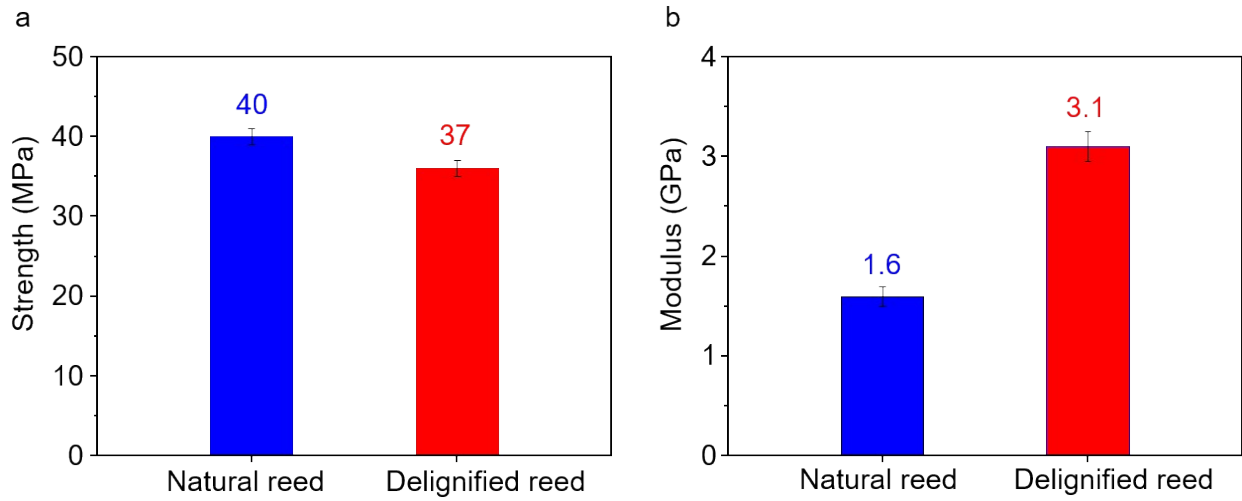


Figure S6. Mechanical properties of the natural and delignified reeds, including the (a) tensile strength and (b) Young's modulus.

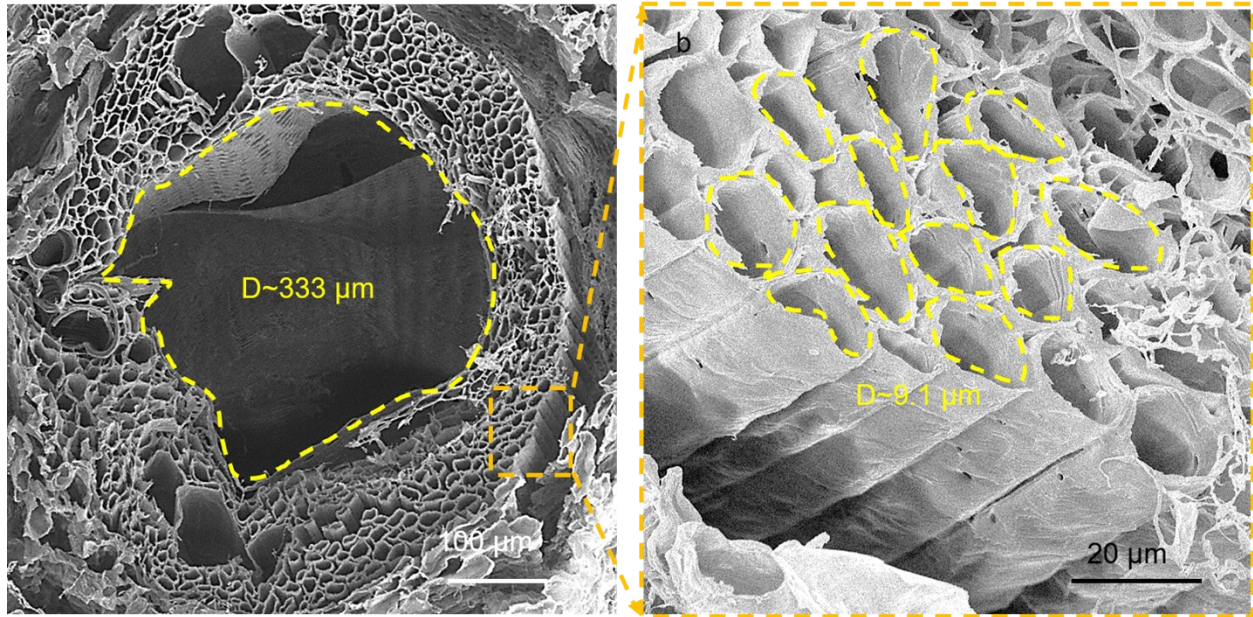


Figure S7. The channel system of delignified reed. The delignified reed features a hierarchically porous structure composed of microchannels, mesochannels, and macrochannels, though the channel structure of the delignified reed is “looser” as a result of the removal of lignin and the increase of void space. In the delignified reed, the macrochannels have an average diameter of $333 \pm 15 \mu\text{m}$ (a), and the microchannels feature an average diameter of $9.1 \pm 1 \mu\text{m}$ (b).

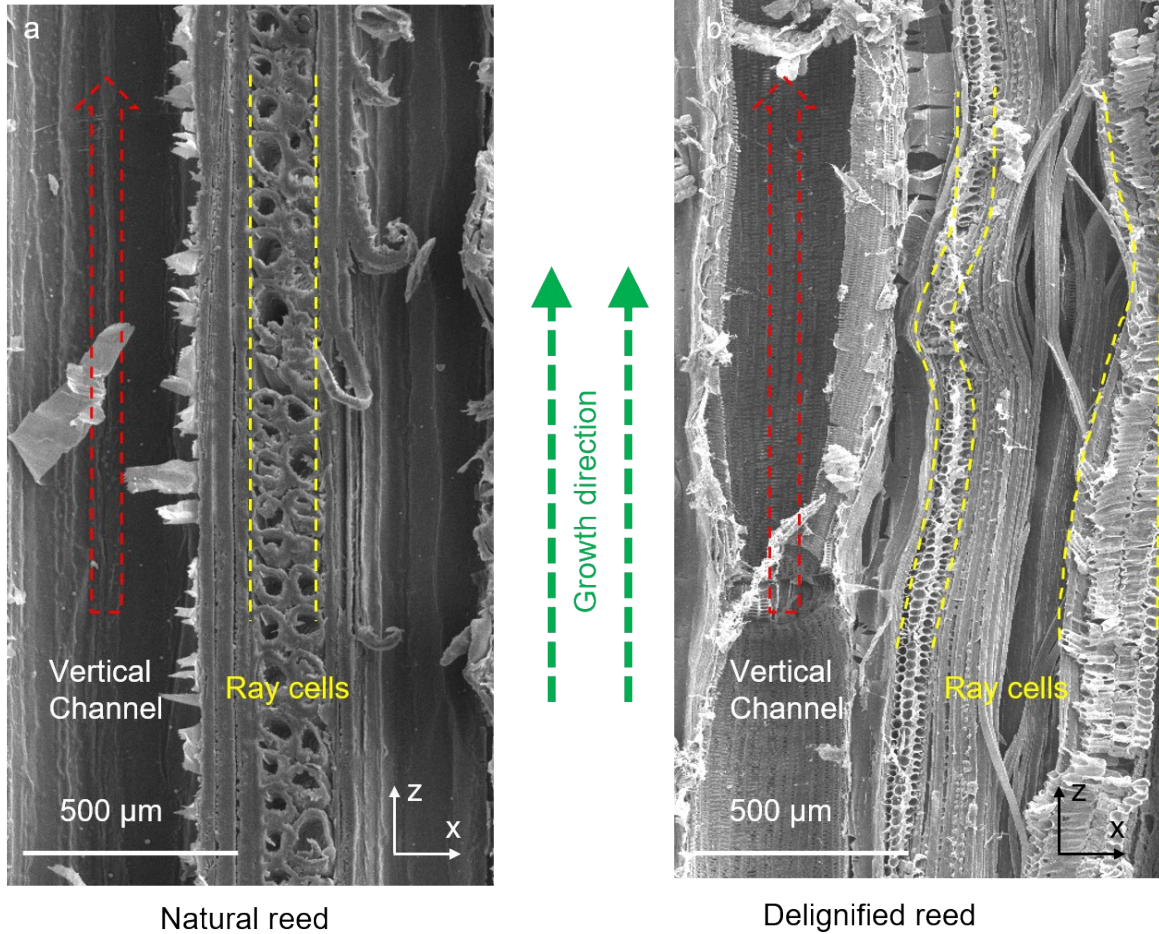


Figure S8. The longitudinal cross-section structure of the (a) natural and (b) delignified reeds. The SEM images illustrate the array of low-tortuosity tube-like channels that run throughout the reed stem along the growth direction, which provides fluidic transport for the plant. Numerous aligned ray cells are arranged radially around the vertical channels, which can enable lateral water transport in the reed stem structure. The delignified reed features much looser structure than the natural reed.

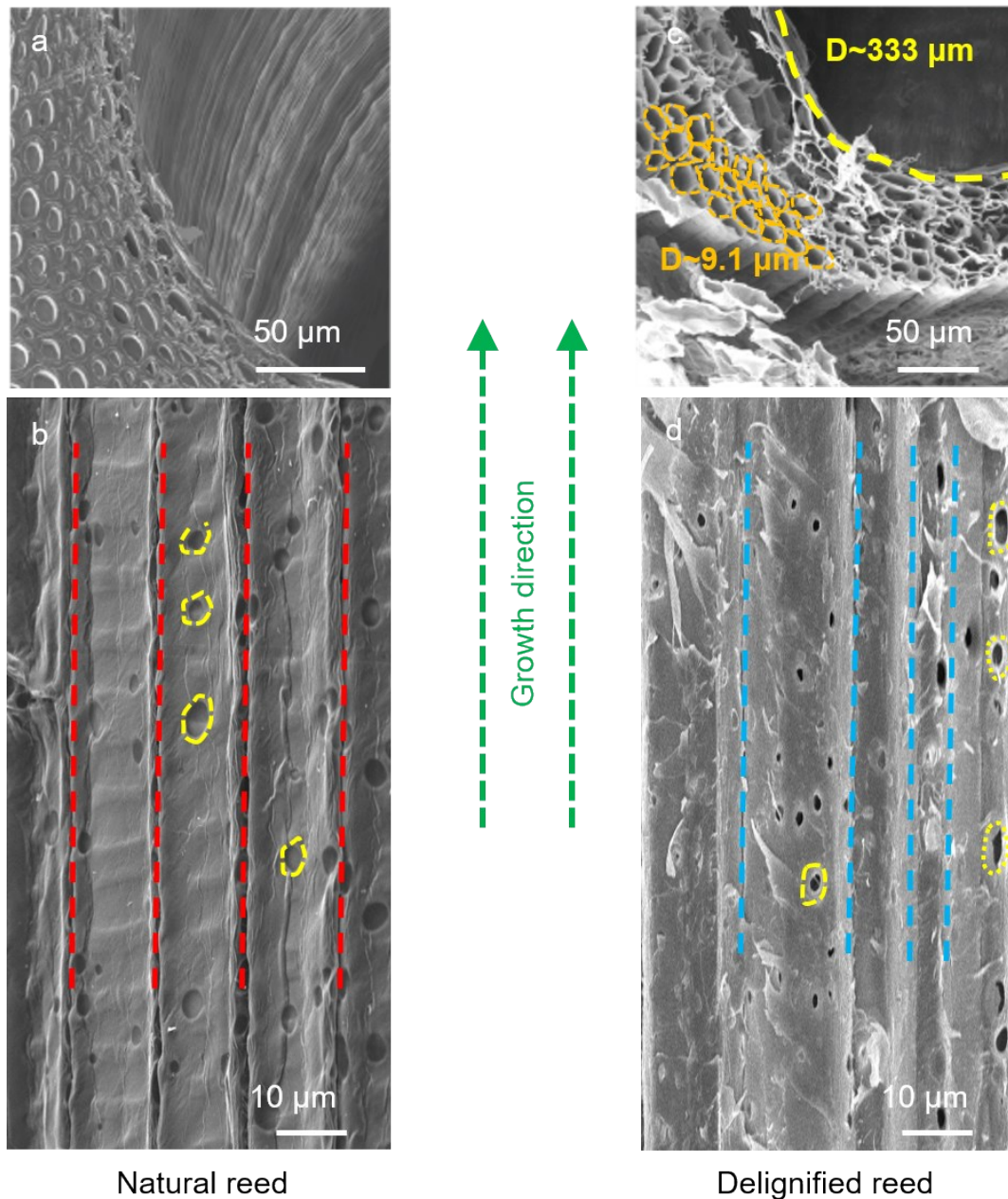


Figure S9. Microchannels of the (a-b) natural and (c-d) delignified reeds, in which a and c are the transverse section, b and d are the longitudinal cross-section. The delignified reed features a looser structure compared with the more compact morphology of the natural reed. Interestingly, many opened pores are present on the microchannel walls of the delignified reed (d), while the pores remain closed in the natural reed (c). The opened pores of the delignified reed can support fluidic transfer between adjacent channels.

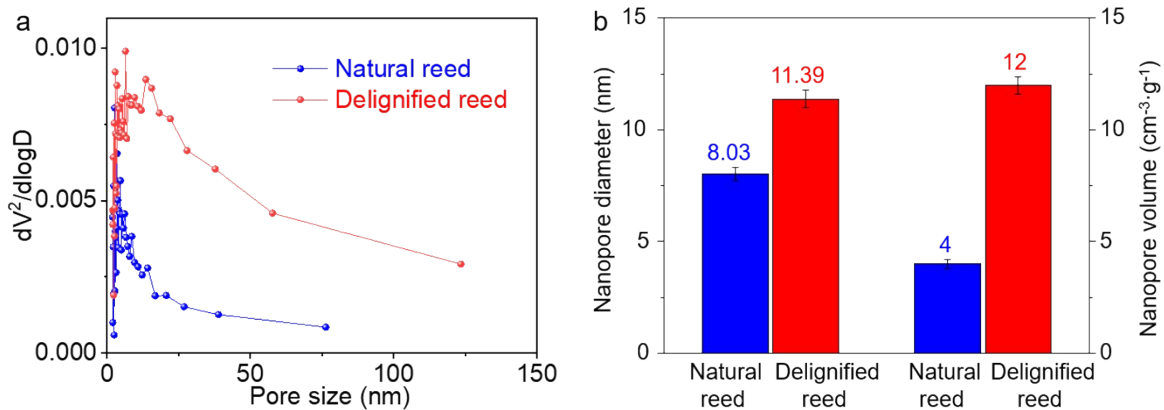


Figure S10. Nano-pore size distribution of the natural and delignified reeds. The results show the delignification treatment creates more nanoscale pores in the delignified reed compared to the natural reed.

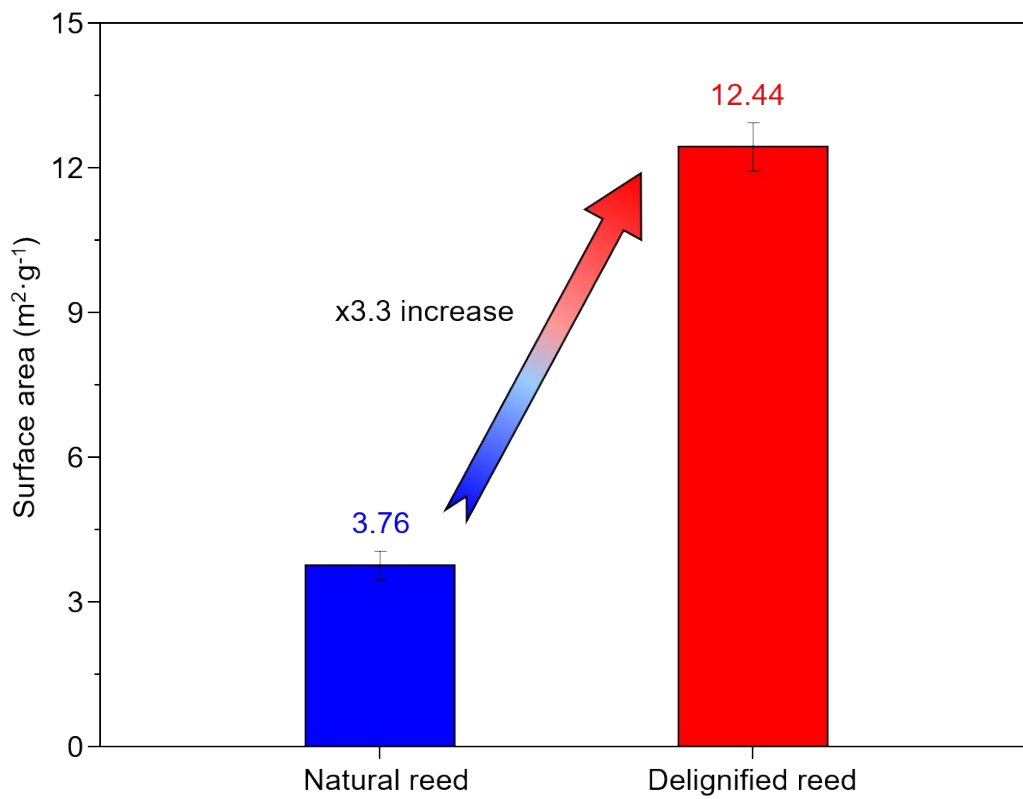


Figure S11. The surface area of the natural and delignified reeds. The delignified reed features an increased surface area, which should promote fluidic transport and evaporation.

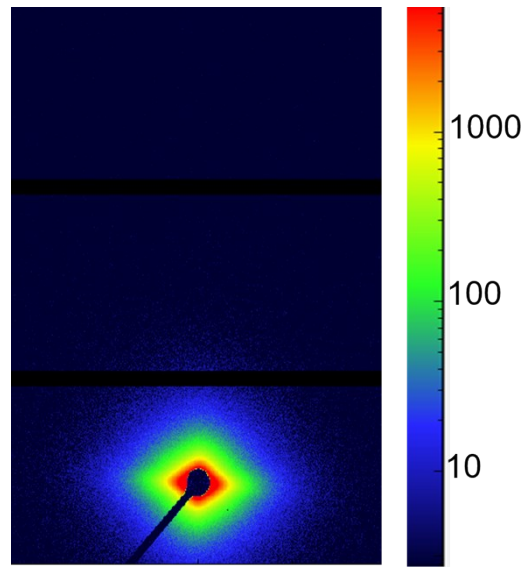


Figure S12. SAXS result of the delignified reed. The diffraction pattern shows an elliptical shape that indicates the aligned structure of cellulose fibrils.

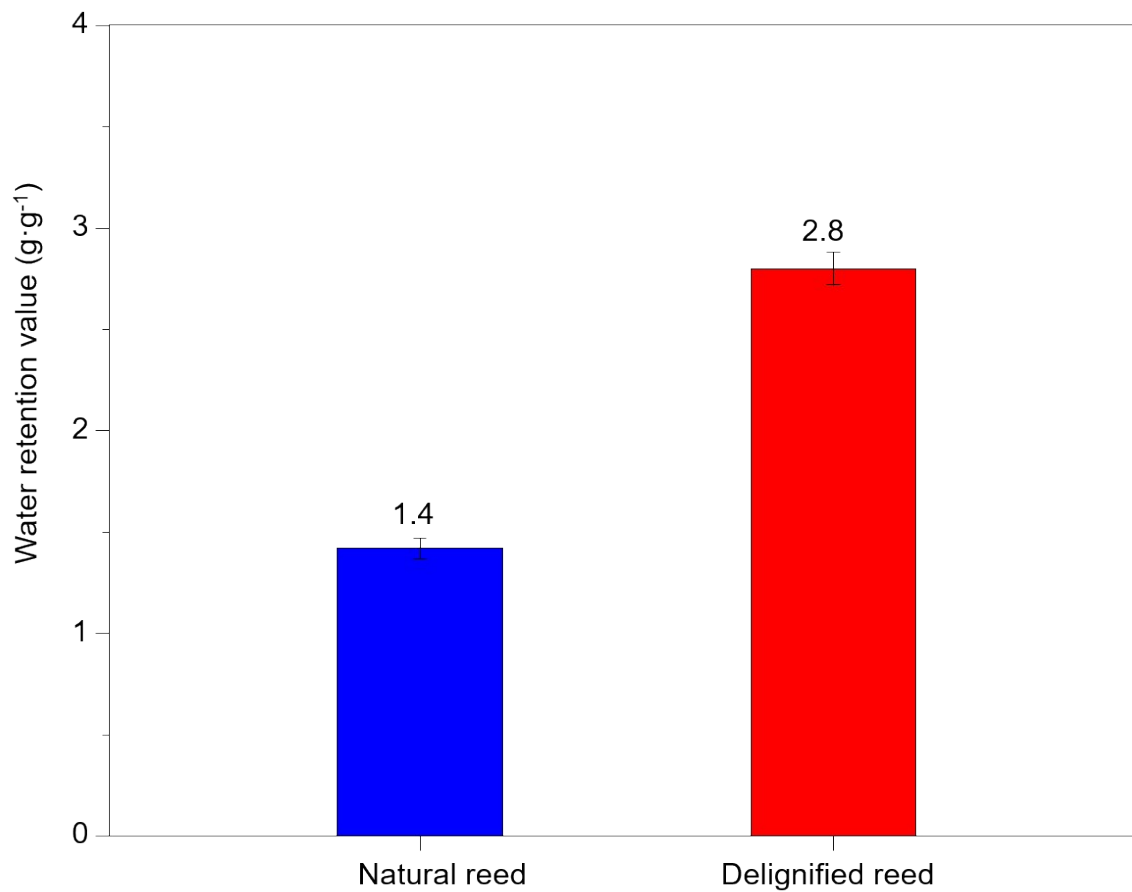


Figure S13. Water retention value of the natural and delignified reeds. Due to the removal of the hydrophobic lignin, the delignified reed features a higher relative content of hydrophilic cellulose, which is responsible for the material's improved water retention value.

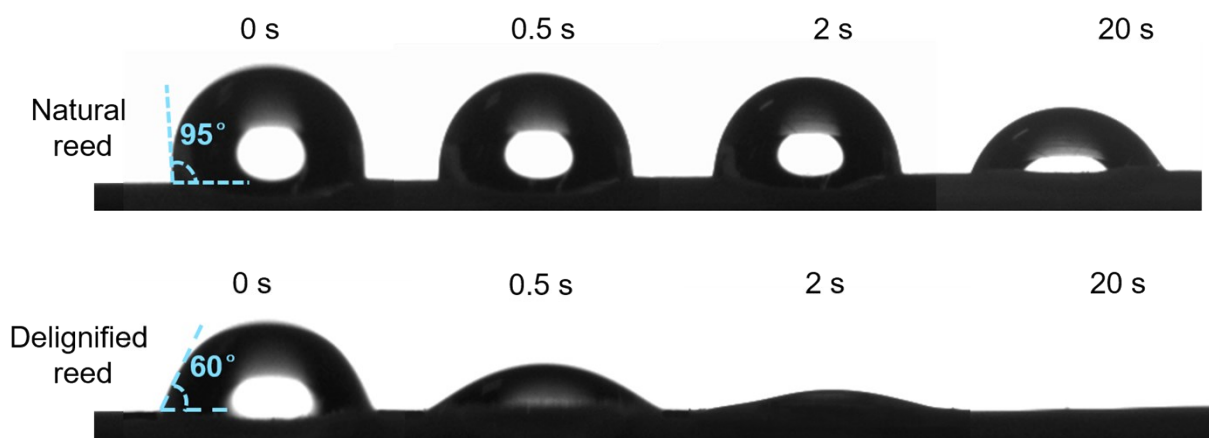


Figure S14. The change of the solution contact angle (CA) of the natural and delignified reeds over time. The delignified reed has a lower CA than the natural reed, with the CA of the delignified reed decreasing to 0° within 20 s. Meanwhile, the natural reed still features a large CA even after 20 s. The different CA values indicate the delignified reed is more hydrophilic than the natural reed.

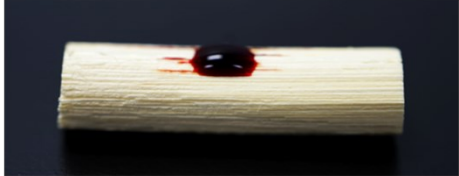

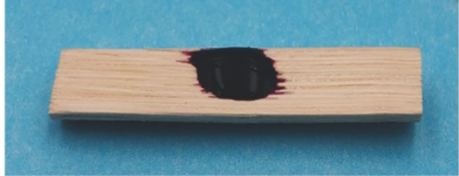
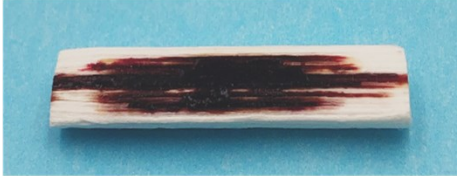
	Natural reed	Delignified reed
Outer surface		
Inner surface		

Figure S15. Photographs of the diffusion and transport of the fluidic solution on the natural and delignified reeds. Both the outer and inner surfaces of the delignified reed demonstrate fast and effective diffusion and transport of a 3% KMnO_4 aqueous solution compared to the natural reed.



Figure S16. The final height of fluid transport along the delignified reed.

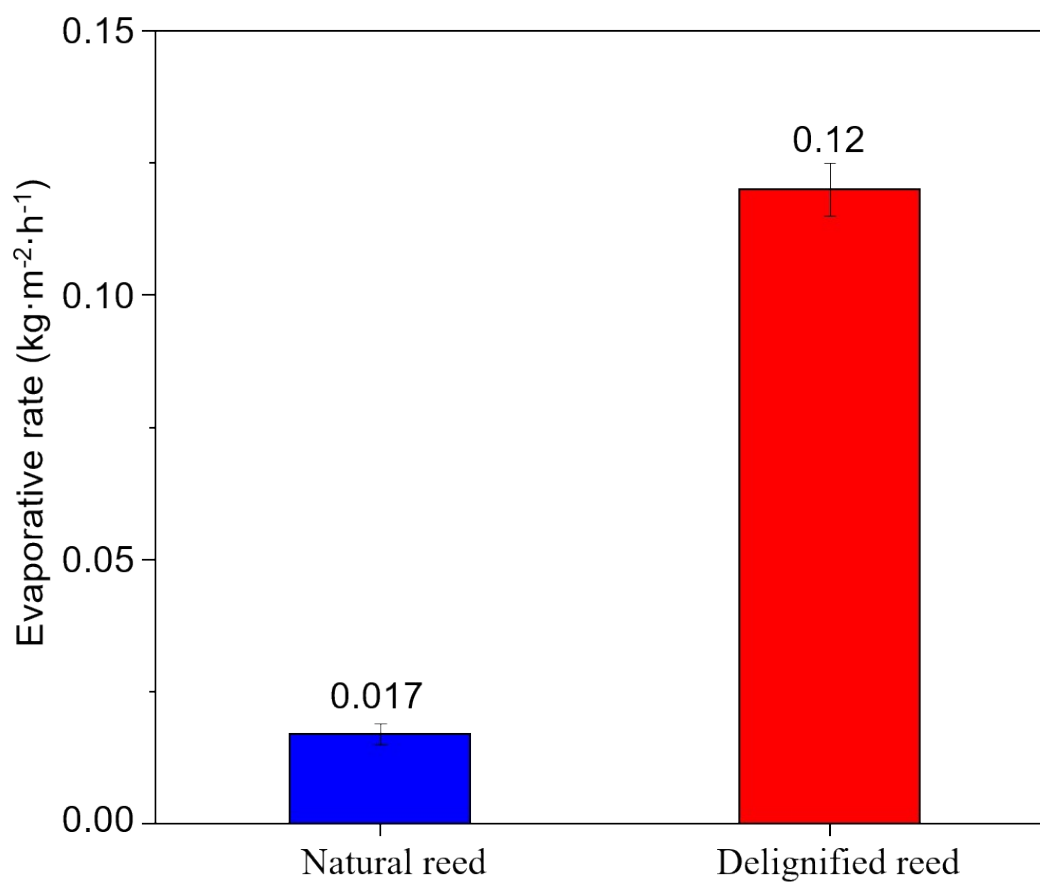


Figure S17. Evaporation rates of the natural and delignified reeds, calculated based on the total outer surface as the evaporative area.

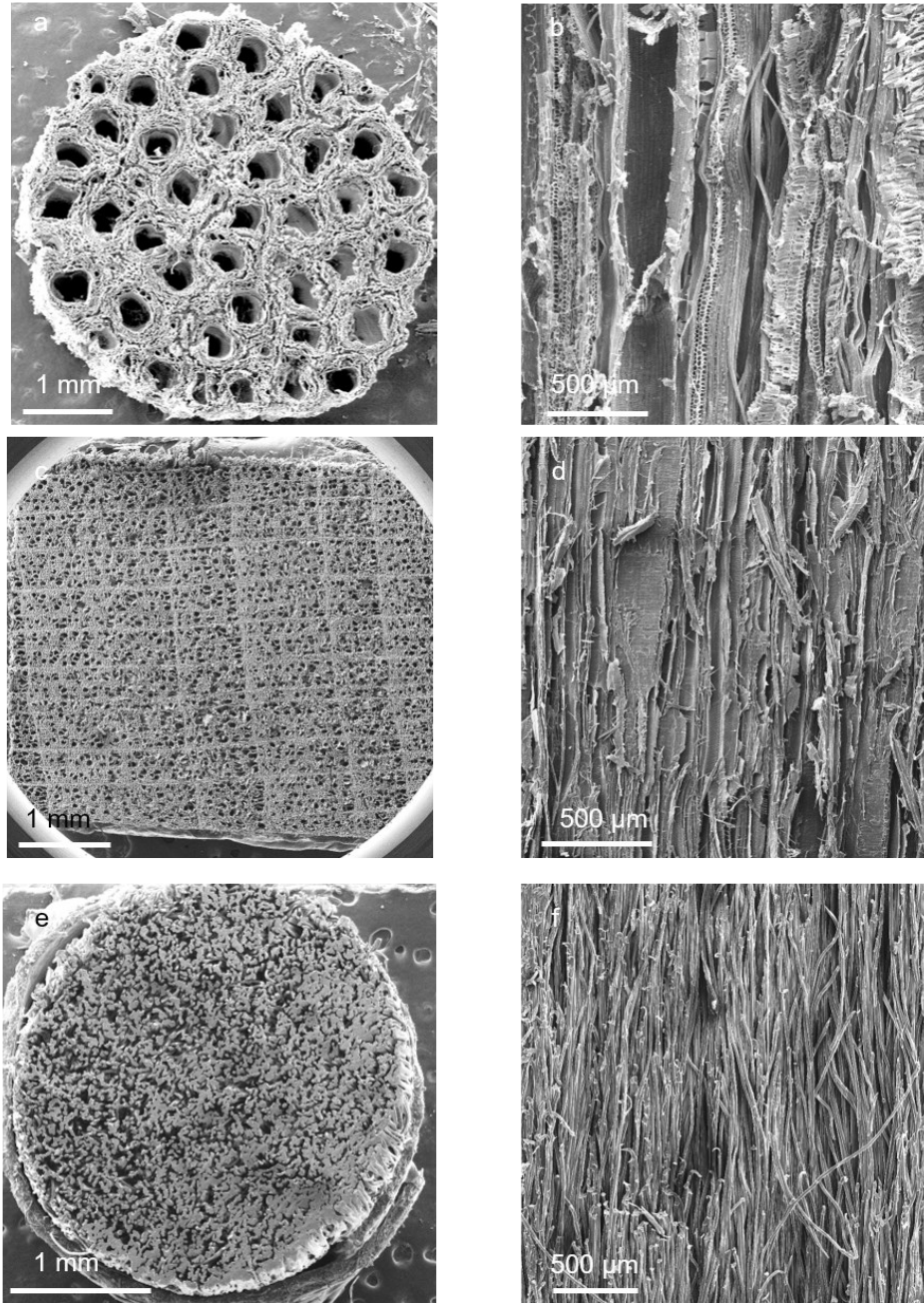


Figure S18. Transverse section and longitudinal cross-section observations of delignified reed, delignified basswood and polyester. (a and b) The delignified reed features hierarchically porous structure, composed of microchannels ($9.1 \pm 1 \mu\text{m}$ diameter), mesochannels ($48 \pm 4 \mu\text{m}$ diameter), and macrochannels ($333 \pm 15 \mu\text{m}$ diameter). The delignified basswood (c and d) and polyester (e and f) feature the relatively uniform-size channels that are $\sim 10\text{--}100 \mu\text{m}$ in diameter, lacking the macro-sized channels ($> 100 \mu\text{m}$ diameter) found in delignified reed.

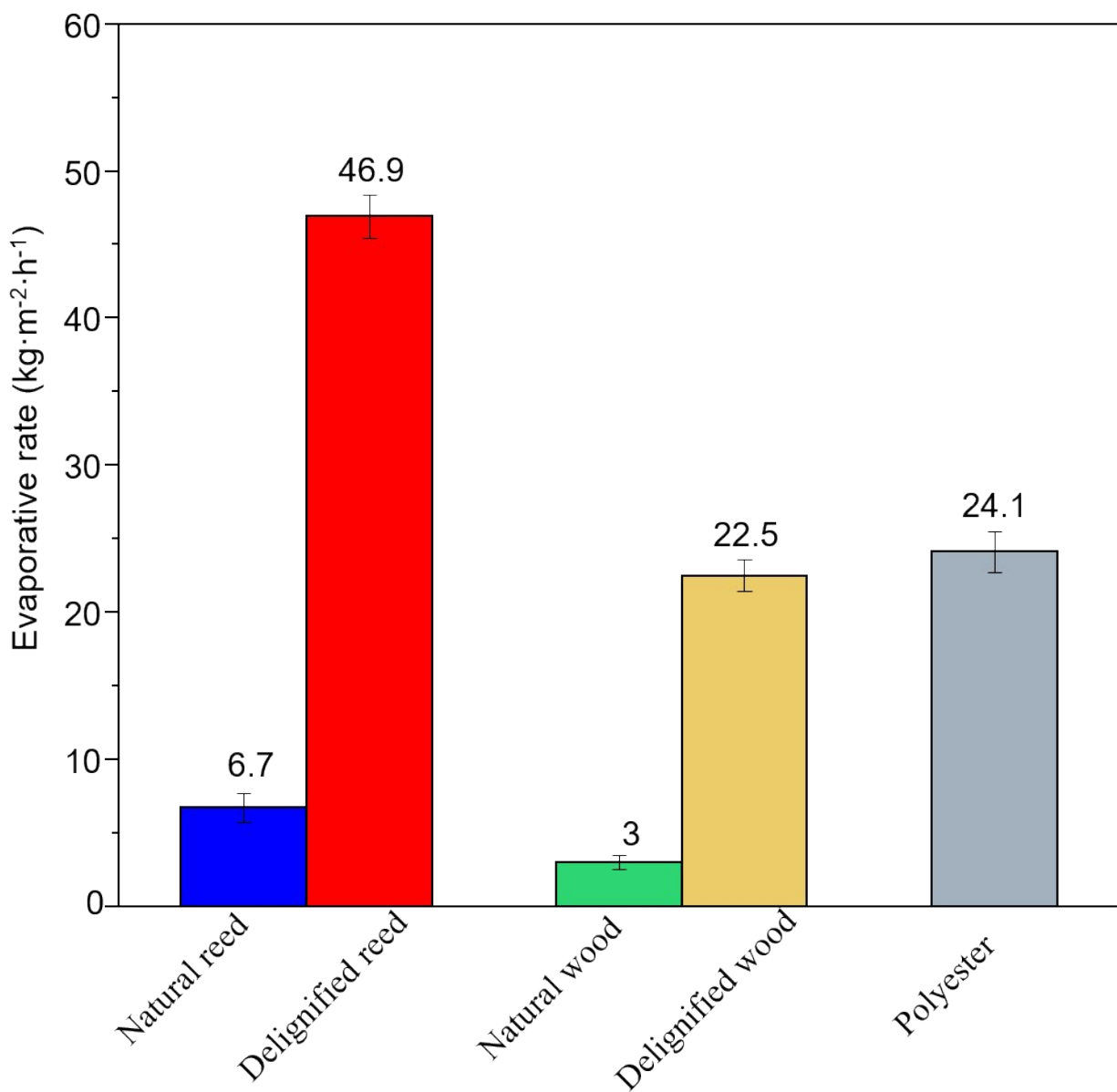


Figure S19. Evaporation rates of different materials. Among them, the delignified reed features the highest evaporation rate. The superior evaporation rate is mainly attributed to the macrochannels (> 100 μm diameter) of the delignified reed, which the wood and polyester evaporators lack.

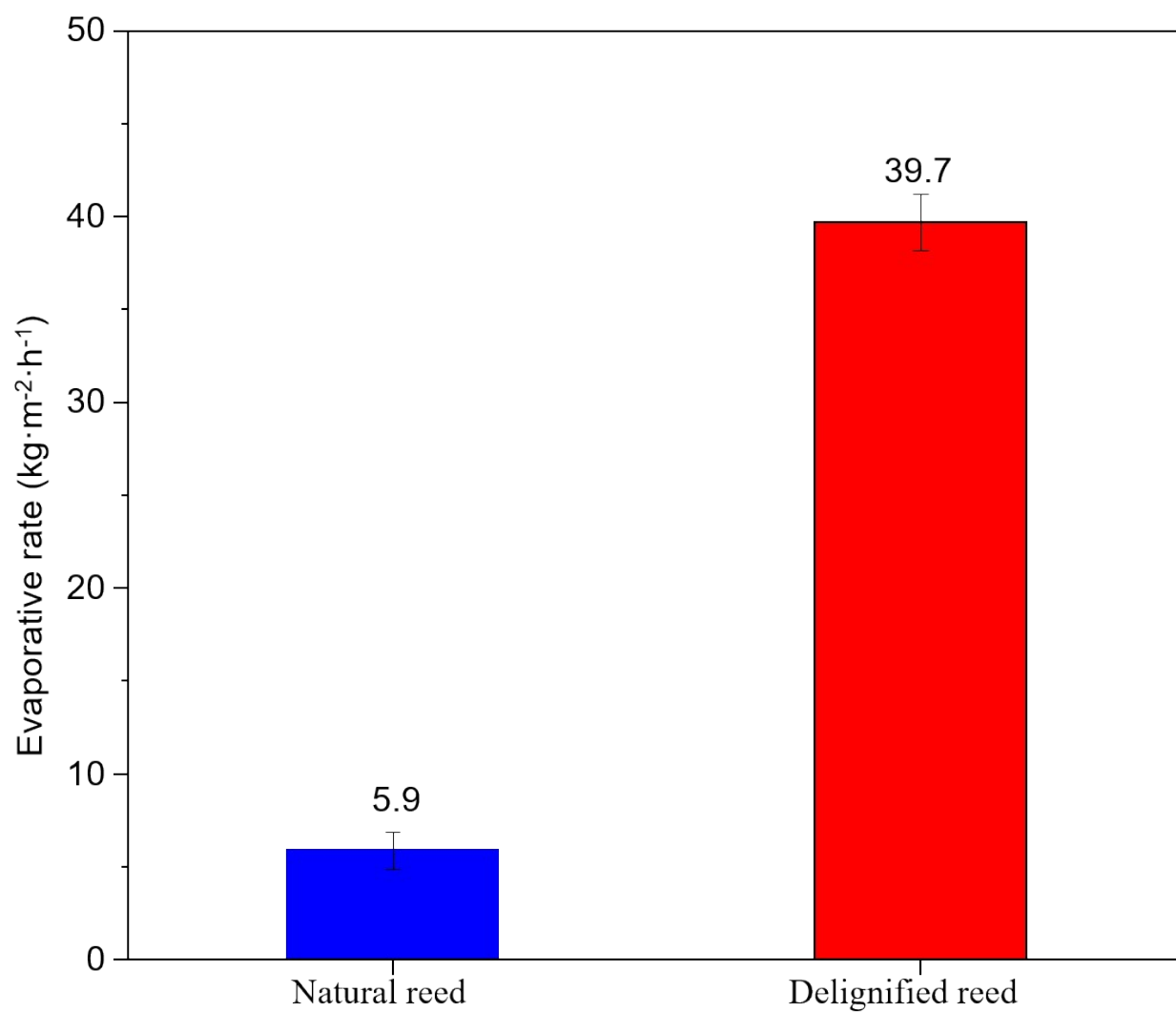


Figure S20. Evaporation rates of the natural and delignified reeds at 40% relative humidity. The delignified reed still shows a much higher evaporation rate than the natural reed at a high humidity.

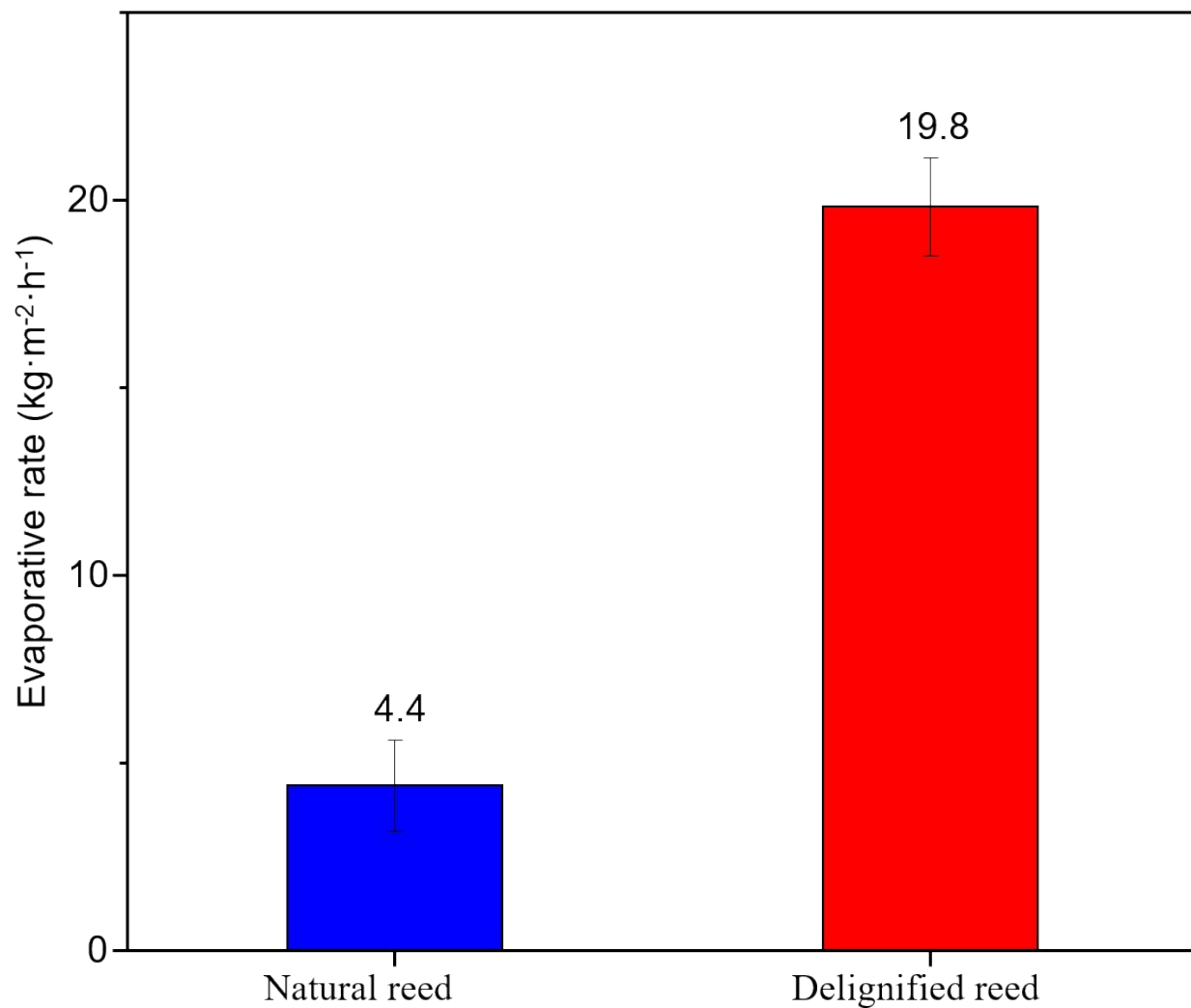


Figure S21. Evaporation rates of the natural and delignified reeds at 80% relative humidity.

Even at a very high humidity of 80%, the evaporation rate of the delignified reed is still much higher than the natural reed.

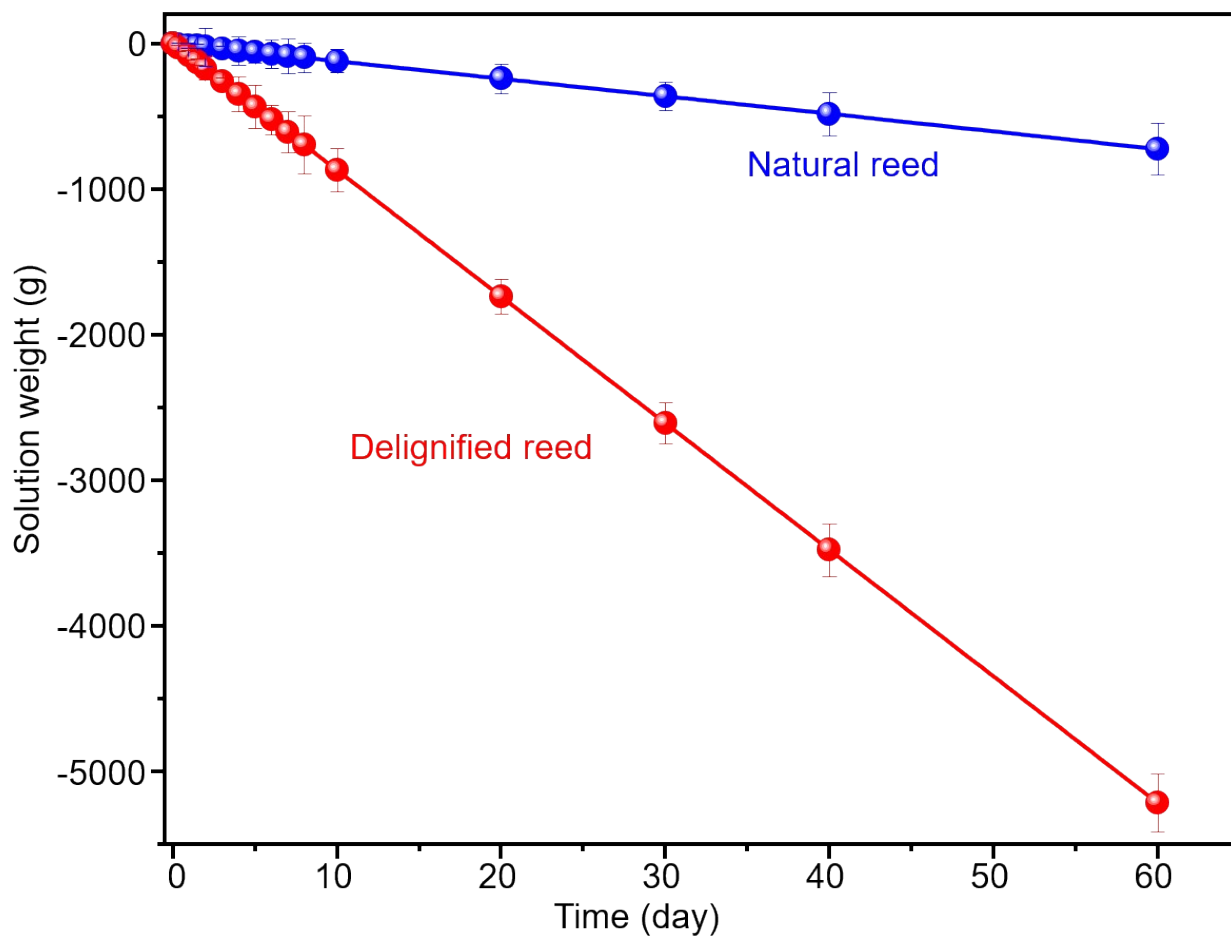


Figure S22. Solution weight loss over 60 days using the natural and delignified reed evaporators.

The results show a linear loss of solution weight over the evaporation time, which is indicative of the stable function of the reed evaporators.

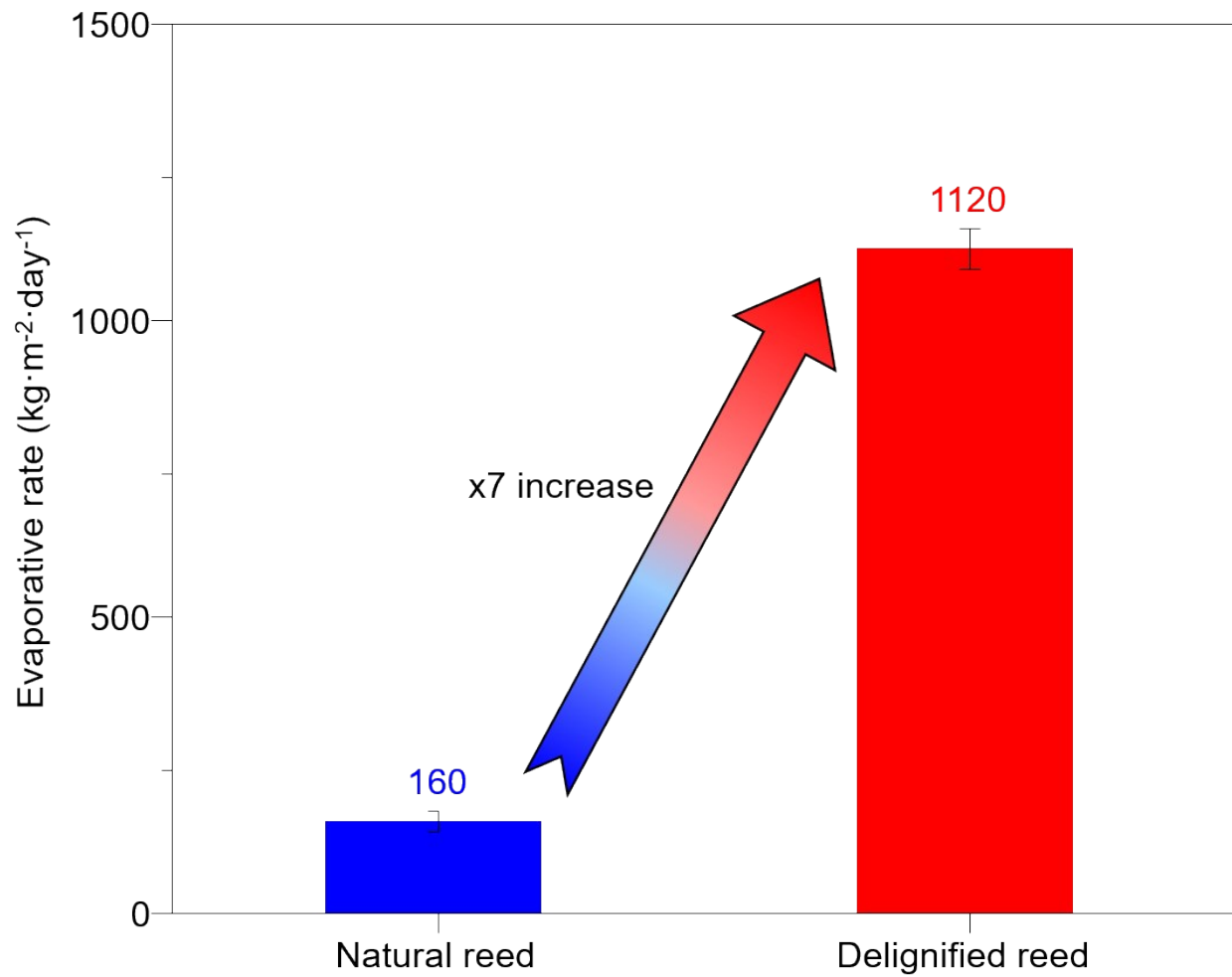


Figure S23. The evaporation rates of the natural and delignified reed after 60 days operation. The delignified reed still shows a 7-times higher evaporation rate than the natural reed.